Articles

Determinants of DNA Mismatch Recognition within the Polymerase Domain of the Klenow Fragment†

Elizabeth H. Z. Thompson,‡ Michael F. Bailey,‡ Edwin J. C. van der Schans,‡ Catherine M. Joyce,§ and David P. Millar*,‡

Department of Molecular Biology, MB-19, The Scripps Research Institute, 10550 North Torrey Pines Road, La Jolla, California 92037, and Department of Molecular Biophysics and Biochemistry, Yale University, New Haven, Connecticut 06520

Received July 9, 2001; Revised Manuscript Received October 3, 2001

ABSTRACT: The Klenow fragment of *Escherichia coli* DNA polymerase I catalyzes template-directed synthesis of DNA and uses a separate 3′−5′ exonuclease activity to edit misincorporated bases. The polymerase and exonuclease activities are contained in separate structural domains. In this study, nine Klenow fragment derivatives containing mutations within the polymerase domain were examined for their interaction with model primer-template duplexes. The partitioning of the DNA primer terminus between the polymerase and 3′−5′ exonuclease active sites of the mutant proteins was assessed by time-resolved fluorescence anisotropy, utilizing a dansyl fluorophore attached to the DNA. Mutation of N845 or R668 disrupted favorable interactions between the Klenow fragment and a duplex containing a matched terminal base pair but had little effect when the terminus was mismatched. Thus, N845 and R668 are required for recognition of correct terminal base pairs in the DNA substrate. Mutation of N675, R835, R836, or R841 resulted in tighter polymerase site binding of DNA, suggesting that the side chains of these residues induce strain in the DNA and/or protein backbone. A double mutant (N675A/R841A) showed an even greater polymerase site partitioning than was displayed by either single mutation, indicating that such strain is additive. In both groups of mutant proteins, the ability to discriminate between duplexes containing matched or mismatched base pairs was impaired. In contrast, mutation of K758 or Q849 had no effect on partitioning relative to wild type, regardless of DNA mismatch character. These results demonstrate that DNA mismatch recognition is dependent on specific amino acid residues within the polymerase domain and is not governed solely by thermodynamic differences between correct and mismatched base pairs. Moreover, this study suggests a mechanism whereby the Klenow fragment is able to recognize polymerase errors following a misincorporation event, leading to their eventual removal by the 3′−5′ exonuclease activity.

The 68 kDa Klenow fragment has been widely used as a model system in the study of DNA polymerases. It is a DNA-dependent DNA polymerase, a proteolytic fragment of the larger DNA Pol I from *Escherichia coli*, that maintains both a polymerase active site and a 3′−5′ exonuclease active site. The latter activity is used in editing of misincorporated nucleotides (*1*). The two active sites are located about 30 Å apart, requiring different binding modes for DNA that nonetheless share a duplex binding groove. Duplex DNA binds at the polymerase active site, whereas only single-stranded DNA binds to the exonuclease site, implying that the Klenow fragment is capable of melting the primer terminus when carrying out an editing reaction on a duplex substrate. It is not completely clear what factors are involved in determining which site a DNA substrate will primarily occupy.

In the minimal kinetic scheme proposed to account for polymerase activity, the initial binding event of a DNA_n substrate (where *n* denotes the length of the nascent strand) to the polymerase is followed by nucleotide binding, a subsequent conformational change of the ternary complex to an "active" polymerizing form, the chemical step of nucleotide incorporation, another conformational change (presumably back to the inactive form), release of pyrophosphate, and, finally, release or translocation of DNA_{n+1} substrate (*2*, *3*). If, instead, the substrate binds at the exonuclease site, an excision reaction takes place and the most recently incorporated base is removed.

At this time, no structures have been solved for the Klenow fragment with DNA bound at the polymerase site, though cocrystal structures are available for other members of the Pol I family, including the large fragment of *Bacillus stearothermophilus* (*Bst*) polymerase, the Klentaq fragment of *Thermus aquaticus* DNA Pol I, and T7 DNA polymerase

† Supported by NIH Grants GM28550 (to C.M.J.) and GM44060 (to D.P.M.).

* Corresponding author: tel, (858) 784-9870; e-mail, millar@scripps.edu.

‡ The Scripps Research Institute.

§ Yale University.

10.1021/bi0114271 CCC: $22.00
Published on Web 12/20/2001

(*4*−*6*). The second of these is actually a series of structures, including two conformations of the polymerase that are thought to correspond to the active and inactive forms in the kinetic scheme. Due to the high degree of homology between these polymerases, these structures may be used to identify residues in the polymerase site of the Klenow fragment that are likely to be in contact with the DNA substrate. Likewise, insights gleaned from the Klenow fragment should be more widely applicable, certainly to other polymerases in the Pol I family and perhaps even to more distantly related polymerases that nevertheless share common structural features (*7*).

Structural data alone often are insufficient to determine the specific functional roles played by amino acid side chains, so other strategies must be pursued to elucidate the structure−function relationships within the polymerase domain. To this end, biochemical studies have identified residues that affect various aspects of polymerase function. This includes protein side chains required for catalysis of the polymerase reaction (*8*, *9*), side chains whose alteration results in mutator and antimutator phenotypes in exonuclease-deficient polymerases (*10*, *11*), residues that determine polymerase specificity for ribo versus deoxyribo sugars (*12*), and residues that are involved in identifying appropriate incoming nucleotide substrates and binding them (*13*, *14*).

If misincorporation events are detected by any means other than the thermodynamic differences between matched and mismatched Watson−Crick base pairs, the DNA duplex suitability for binding at the polymerase or 3′−5′ exonuclease site must be evaluated prior to nucleotide incorporation. Presumably, the suitability for each site is related to whether the DNA contains a mismatched base pair resulting from a previous misincorporation event, though whether the evaluation is based on geometrical constraints or specific interactions, such as hydrogen bonds between duplex and protein, has not been clarified. Since the primer-template binds as a duplex at the polymerase site, whereas the melted primer strand alone binds at the exonuclease active site, mismatches in the duplex could only be identified by interactions with amino acid residues in the polymerase domain. The details of this recognition mechanism remain unknown, however, as there are no structures available for DNA polymerases bound to DNA substrates containing mismatched base pairs.

In this study, we employ site-directed mutagenesis and time-resolved fluorescence anisotropy to identify amino acid residues within the polymerase domain of the Klenow fragment that enable the enzyme to discriminate between DNA duplexes containing correct or mismatched base pairs. Previous studies demonstrated that the fluorescence anisotropy behavior of a dansyl probe incorporated into the DNA duplex could be used to measure the relative partitioning of that probe between the polymerase and exonuclease domains of the Klenow fragment (*15*). This technique has been applied to the wild-type Klenow fragment bound to various duplex DNAs, including those with mismatched base pairs and extrahelical base bulges, and to derivatives of the Klenow fragment with mutations in the 3′−5′ exonuclease domain (*16*−*19*). Here we investigate the effect of mutations in specific protein side chains in the polymerase domain and quantify the resulting changes in the equilibrium distribution of duplex DNA substrates, either matched or mismatched, between the separate polymerase and 3′−5′ exonuclease sites.

Table 1: Duplex DNA Sequences[a]

PT0	5′-TCGCAGCCG**X**CAAAATG AGCGTCGGCAGTTTTACATATAGCCGA-5′
PT1	5′-TCGCAGCCG**X**CAAAATG AGCGTCGGCAGTTTTA$_{G}$ATATAGCCGA-5′
PT2	5′-TCGCAGCCG**X**CAAAATG AGCGTCGGCAGTTTT$_{GG}$ATATAGCCGA-5′
PT4	5′-TCGCAGCCG**X**CAAAATG AGCGTCGGCAGTT$_{CCTT}$ATATAGCCGA-5′

[a] **X** indicates a modified uridine residue with an attached dansyl label. The position of the dansyl label was optimized in previous experiments such that the dansyl experiences different local environments when the primer terminus is bound at the two active sites (*15*, *16*). Subscripted bases in the sequence indicate mismatches between the primer and template strands.

MATERIALS AND METHODS

Oligonucleotide Synthesis and Labeling. Oligonucleotides were synthesized on an automated DNA synthesizer (Pharmacia Gene Assembler Plus) using standard β-cyanoethyl phosphoramidite chemistry and then purified by reverse-phase HPLC using an acetonitrile/triethylammonium acetate eluant system.

Dansyl-labeled oligonucleotides were prepared through the use of a protected 5-(propylamino)deoxyuridine residue, introduced during automated synthesis. The modified residue was then deprotected and labeled with dansyl chloride, as described previously (*20*).

Fluorescein-labeled oligonucleotides were prepared through the use of a six-carbon amino linker incorporated at the 5′ end. The 5′-aminooligonucleotide was reacted with 5-carboxyfluorescein succinimidyl ester in a buffer of 0.15 M sodium bicarbonate (pH 8.3) and left in the dark overnight. Unreacted dye was removed by gel filtration chromatography, and the dye-labeled oligonucleotide was purified by gel electrophoresis.

Five oligonucleotide sequences were used for time-resolved fluorescence anisotropy measurements (Table 1): a 17-nt dansyl-labeled primer strand and four different 27-nt unlabeled template strands. The four template strands were combined with the primer to produce four duplexes, designated PT0, PT1, PT2, and PT4, where the number refers to the number of terminal mismatches. Duplex DNA samples were annealed by mixing 3 μM primer strand and 3.6 μM template strand in our standard buffer [50 mM Tris (pH 7.5) and 3 mM $MgCl_2$]. The samples were heated to 80 °C for 10 min and allowed to cool slowly to room temperature. The duplex used for exonuclease site binding titrations comprised the same oligonucleotide sequences as in PT4, with the exception that the primer strand was 5′ end labeled with fluorescein and the modified base (denoted **X** in Table 1) was replaced by thymine. The fluorescein-labeled duplex was prepared by annealing 8 μM primer and template strands as described above.

Preparation and Purification of Mutant Polymerases. Single amino acid changes in the polymerase domain of the Klenow fragment were investigated in an exonuclease-deficient background. Exonuclease activity was abolished by the presence of the previously reported D424A mutation (21). Construction of plasmids for R841A, N845A, Q849A, R668A, N675A, and R835L has been described elsewhere (*9*, *11*), and the plasmid encoding the R836A mutation was similarly produced. The K758A and N675A/R841A plasmids

were produced by site-directed mutagenesis of preexisting plasmids (D424A and D424A/R841A, respectively), using slight modifications of the QuikChange SDM kit from Stratagene. Proteins were heat-induced in the host strain CJ376 and were purified as described elsewhere (*22*). The naming convention used for mutant derivatives is as follows: the residue number is preceded by the one-letter code for the wild-type amino acid and followed by the code for the mutant amino acid.

Circular Dichroism. To determine whether polymerase site mutations had deleterious effects on the structure of the Klenow fragment and to assess the extent of nonfolded protein, the far-UV CD spectrum was collected for each mutant protein. Proteins were examined at a concentration of 2.5 μM in the standard binding buffer [50 mM Tris (pH 7.5) and 3 mM $MgCl_2$]. Due to the presence of Tris in the buffer, data were only collected from 200 to 250 nm.

Exonuclease Site Binding Titrations. Titrations to probe the effect of polymerase site mutations on DNA binding at the 3′−5′ exonuclease site were performed with a fluorescein end-labeled DNA duplex substrate containing four consecutive mismatched base pairs. Aliquots of protein were added to a solution of labeled duplex, and the progress of the titration was monitored by the resultant steady-state anisotropy value. Fluorescence was excited at 490 nm and monitored at 520 nm on an SLM Aminco 8100 spectrofluorometer. The steady-state anisotropy was determined using the L-format setup, *G* factor correction, integration time of 1 s, and 10 replicates per measurement. Standard deviations of the measurements were typically 0.001−0.002. All measurements were performed at 20 °C.

Time-resolved fluorescence anisotropy data show that a substrate containing four consecutive mismatches was bound predominantly (≥80%) at the exonuclease site (see below). For this reason, steady-state titration data were fit to a single-site binding model, where DNA bound only at the exonuclease site. For this model, the steady-state anisotropy of a mixture of DNA and protein can be expressed as in the equation:

$$r = r_F\left(\frac{f_F Q_F}{f_F Q_F + f_B Q_B}\right) + r_B\left(\frac{f_B Q_B}{f_F Q_F + f_B Q_B}\right) \quad (1)$$

where r is the observed anisotropy, r_F is the steady-state anisotropy of the free DNA, Q_F is the quantum yield of the fluorescent probe in the free DNA, and f_F is the equilibrium fraction of free DNA in the mixture; r_B, Q_B, and f_B are the corresponding quantities for the bound DNA.

Using the equality $f_F + f_B = 1$ and introducing the ratio $R = Q_B/Q_F$, eq 1 may be written in the form of the equation:

$$r = \frac{(Rr_B - r_F)f_B + r_F}{(R-1)f_B + 1} \quad (2)$$

In both eqs 1 and 2, the equilibrium fraction of bound DNA is given by the formula in the equation:

$$f_B = \{(K_{D,exo} + [DNA] + [KF]) - \sqrt{(K_{D,exo} + [DNA] + [KF])^2 - 4[DNA][KF]}\}/(2[DNA]) \quad (3)$$

where $K_{D,exo}$ is the dissociation constant for DNA bound to the 3′−5′ exonuclease site and [DNA] and [KF] are the total concentrations of DNA and the Klenow fragment, respectively.

Titration data were fit to eqs 2 and 3 using a Marquardt nonlinear least squares algorithm. The anisotropy values for the fluorescein-labeled DNA in the free and bound states were fixed during fitting ($r_F \cong 0.09$ and $r_B = 0.35$). Likewise, the ratio of the quantum yields of the free and bound states was fixed at previously determined values ($R = 1.6$). As some protein preparations contained an inactive fraction incapable of binding DNA, the total protein concentration in eq 3 was replaced by x[KF], where x is the fraction of active protein. Titration data were fit with $K_{D,exo}$ and x as fitting parameters.

The Gibbs free energy of binding the DNA substrate to the exonuclease site was calculated according to the equation:

$$\Delta G^\circ_{exo} = RT \ln K_{D,exo} \quad (4)$$

where R is the gas constant and T is the absolute temperature.

The change in the free energy of exonuclease site binding resulting from a mutation of the protein was calculated from the equation:

$$\Delta\Delta G^\circ_{exo} = RT \ln\left[\frac{K_{D,exo}(\text{mutant})}{K_{D,exo}(\text{wild type})}\right] \quad (5)$$

Time-Resolved Fluorescence Anisotropy. The fractional occupancies by a DNA substrate of the polymerase and 3′−5′ exonuclease active sites of the Klenow fragment can be measured using the distinguishable fluorescence anisotropy decay behavior exhibited by a dansyl-labeled DNA substrate bound at each of the two active sites (*15*, *16*).

Fluorescence decay curves were measured by the time-correlated single-photon counting method. The fluorescence of the dansyl probe was excited at 318 nm by vertically polarized, frequency-doubled output from a cavity-dumped, mode-locked, synchronously pumped DCM dye laser (Coherent 702). The resulting emission was measured at 530 nm at right angles to the excitation. Horizontally and vertically polarized emissions were measured, with the emission polarizer alternating every 30 s, and a polarization scrambler was placed in the emission beam at the input of the monochromator to eliminate polarization bias of the grating. The fluorescence transmitted by the monochromator was detected by a microchannel plate photomultiplier (Hamamatsu R2809). Decays were recorded in 512 channels using a time increment of 88 ps per channel. All measurements were performed at 20 °C. To ensure that data were collected only for samples in which the DNA substrate was completely bound by protein, measurements were made with increasing protein concentrations until there was no difference between subsequent data sets.

The time-dependent fluorescence anisotropy was calculated from the vertically and horizontally polarized components of the emission [$I_{||}(t)$ and $I_\perp(t)$, respectively], according to the equation:

$$r(t) = \frac{I_{||}(t) - I_\perp(t)}{I_{||}(t) + 2I_\perp(t)} \quad (6)$$

Anisotropy decays were globally analyzed with a two-state model of exposed and buried dansyl probes, corresponding to DNA primer-template bound at the polymerase and exonuclease sites, respectively. The details of the model and the data fitting procedure have been described in previous studies (*16*, *19*, *23*). The quality of the two-state model fit was assessed from the value of the global χ^2 parameter and the local χ^2 values for each data set.

In the analysis, the spectroscopic parameters describing each probe environment are globally linked across all data sets, while the fraction of buried dansyl probes (denoted x_b) is locally optimized for each data set. The fraction of exposed probes (x_e) is then obtained for each data set from the equality $x_b + x_e = 1$.

Due to the discrepancy between the probe fluorescence lifetime and the rotational correlation time for tumbling of the DNA/protein complex, the latter was poorly determined, resulting in poor fits of some curves to a globally determined value of 57 ns. Better fits were obtained when the tumbling time was allowed to be a local variable, determined separately for each anisotropy curve. This modification of the previously described curve-fitting protocol (*16*) had no significant impact on the fraction of buried probes recovered from a given anisotropy decay.

Calculation of Free Energy Changes. The equilibrium constant describing partitioning of DNA between the polymerase site and the exonuclease site, K_{pe}, was computed as in the equation:

$$K_{pe} = \frac{[\text{exonuclease complex}]}{[\text{polymerase complex}]} = \frac{x_b}{x_e} \quad (7)$$

where x_b and x_e are the fractions of buried and exposed dansyl probes recovered from analysis of the fluorescence anisotropy decay.

The Gibbs free energy of partitioning is defined in the equation:

$$\Delta G^\circ_{pe} = -RT \ln K_{pe} \quad (8)$$

The change in the free energy of partitioning due to a mutation of the protein is calculated as in the equation:

$$\Delta\Delta G^\circ_{pe} = -RT \ln\left[\frac{K_{pe}(\text{mutant})}{K_{pe}(\text{wild type})}\right] \quad (9)$$

The free energy of partitioning can also be expressed as a difference in the Gibbs free energy of binding the DNA substrate at the polymerase site, ΔG°_{pol}, or exonuclease site, ΔG°_{exo}, as in the equation:

$$\Delta G^\circ_{pe} = \Delta G^\circ_{exo} - \Delta G^\circ_{pol} \quad (10)$$

which can be rearranged to give

$$\Delta G^\circ_{pol} = \Delta G^\circ_{exo} - \Delta G^\circ_{pe} \quad (11)$$

The effect of a mutation on the energetics of polymerase site binding of DNA was assessed in terms of $\Delta\Delta G^\circ_{pol}$, calculated according to the equation:

$$\Delta\Delta G^\circ_{pol} = \Delta\Delta G^\circ_{exo} - \Delta\Delta G^\circ_{pe} \quad (12)$$

where $\Delta\Delta G^\circ_{exo}$ and $\Delta\Delta G^\circ_{pe}$ are given by eqs 5 and 9, respectively.

RESULTS

Mutant Derivatives of the Klenow Fragment. Nine mutant derivatives of the Klenow fragment were examined. These contained mutations in amino acid side chains located within the polymerase domain: R668, N675, K758, R835, R836, R841, N845, and Q849. The wild-type residues were replaced by alanine (or, in one case, leucine) in order to eliminate potentially important side chain interactions. Eight single site mutations and one dual site mutant (N675A/R841A) were examined. Structural data for DNA polymerases homologous to the Klenow fragment show the side chains corresponding to R668, N675, R841, N845, and Q849 in proximity to the duplex DNA substrate at the polymerase site (*4*−*6*, *24*), as illustrated in Figure 1B, while R835 and R836 might be appropriately positioned to interact with the single-stranded template. Previous biochemical studies have also implicated the R668, R841, and N845 side chains in interactions with substrates at the polymerase active site and the N845 side chain in fidelity (*8*, *9*, *11*). The K758 side chain makes no contacts with the primer or template strands of the DNA substrate (Figure 1, and therefore serves as a control.

In addition to the polymerase domain mutations, the Klenow fragment derivatives in this study also contained the 3′−5′ exonuclease-deficient D424A mutation to prevent degradation of the DNA substrates during fluorescence measurements. For simplicity, each protein is described by the polymerase domain mutation only. Accordingly, the D424A control is referred to as wild type, and N675A refers to the double mutation D424A/N675A. It should also be noted that the "double" mutant (N675A/R841A) is more properly a triple mutant that contains the additional D424A mutation.

CD spectra were obtained for each single mutant protein and compared with the spectrum of the wild-type protein as a check for gross misfolding. In all cases, CD spectra of the mutant proteins were identical in shape to that of the wild-type protein, indicating similar global folds (data not shown).

Exonuclease Site Binding Titrations. Mutant Klenow fragment derivatives were first assayed for their ability to bind DNA at the 3′−5′ exonuclease site. Although the mutated side chains are located within the polymerase domain, some are within the part of the DNA binding site that is common to both polymerase and exonuclease binding modes (Figure 1A). Accordingly, it was important to determine whether the effects of the chosen mutations could also alter the exonuclease mode of binding. Such effects would complicate the analysis of what are intended to be polymerase site mutations.

Exonuclease site binding titrations were carried out with a fluorescein 5′ end labeled primer-template duplex containing four consecutive base mismatches at the 3′ end of the primer strand. Measurements of active site partitioning (presented below) indicate that this substrate binds predominantly (≥80%) at the exonuclease site in all Klenow fragment derivatives. The relatively high quantum yield of fluorescein facilitated measurements at low DNA concentrations, necessary to determine the equilibrium dissociation constants for the various DNA/protein complexes.

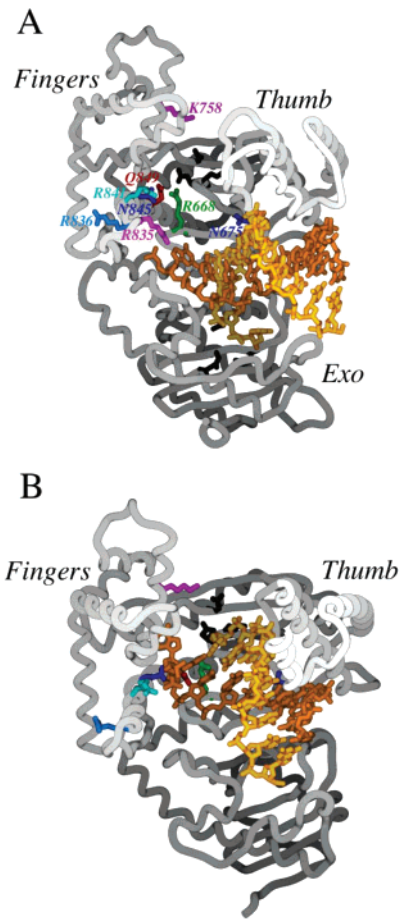

FIGURE 1: Comparison of polymerase complex structures with DNA duplex substrates bound at the 3′−5′ exonuclease (editing) and polymerase sites. The exonuclease complex (A) corresponds to a Klenow fragment editing complex (*24*; PDB file 1KLN). The polymerase complex (B) is a binary complex of the large fragment of *B. stearothermophilus* (*Bst*) DNA polymerase with DNA (*4*; PDB file 2BDP). This structure was chosen because the complex was formed simply by mixing the DNA primer-template and the polymerase, as were the complexes in our study. Nevertheless, comparison of the *Bst* polymerase complex with the binary complex of Klentaq and DNA, formed by loss of the nucleotide from a ternary complex (*5*), and also with the ternary complexes of Klentaq and T7 DNA polymerase (*5*, *6*) reveals very similar positioning of the DNA duplex in all four cases. Both panels show similar orientations, viewed from above the polymerase domain cleft, with the primer and template DNA strands in light and dark shades of gold, respectively. The carboxylate side chains at the polymerase active sites of both polymerases, and the 3′−5′ exonuclease active site of the Klenow fragment, are shown in black (the *Bst* polymerase does not have 3′−5′ exonuclease activity). In the Klenow fragment editing complex (A), the eight side chains mutated in this work are shown. In the *Bst* polymerase complex (B), seven of the residues equivalent to the Klenow fragment side chains are shown, using the same color scheme as in (A). The single exception is Arg835, which is not well conserved in the Pol I family; the equivalent side chain in the *Bst* polymerase is Val783, whose side chain is oriented differently from the Arg side chain in the Klenow fragment. For clarity, 27 residues at the tip of the thumb of the *Bst* polymerase are not shown. This figure was created using SPOCK (*29*).

Binding titrations were performed by titrating a fixed concentration (6 or 20 nM) of fluorescein-labeled DNA with a given Klenow fragment mutant derivative (Figure 2). With inclusion of the weighting factor for protein concentration (see Materials and Methods), all curves were fit satisfactorily. An example of the quality of the fits may be seen in Figure 2. The $K_{D,exo}$ value obtained for the wild-type Klenow fragment is 33 nM. The corresponding values for the mutant proteins (Table 2) are similar. Consequently, the $\Delta\Delta G°_{exo}$ values for the mutant proteins are small in magnitude (Table 2). These results confirm that the chosen mutations within the polymerase domain do not significantly perturb binding of DNA to the exonuclease site.

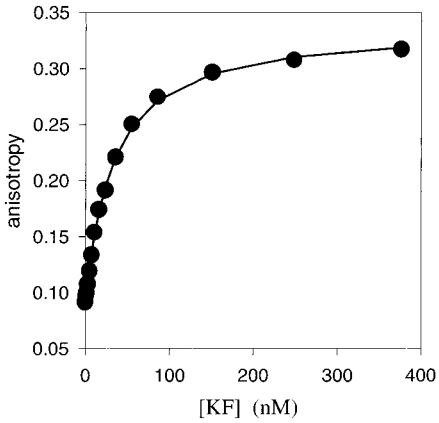

FIGURE 2: Exonuclease site binding titrations. Titrations were performed with quadruply mismatched DNA to ensure complete exonuclease site binding. The solid circles are experimental points for the wild-type Klenow fragment. The smooth line is a best-fit curve. Fits were generated with the program SigmaPlot, based on the difference in anisotropy exhibited by a fluorescein-labeled DNA substrate when free or bound at the exonuclease site (eqs 2 and 3 in Materials and Methods).

Table 2: Effect of Mutations on Exonuclease Site Binding of DNA

protein	K_D value for exonuclease site (nM)[a]	$\Delta\Delta G°_{exo}$ (kJ mol^{-1})[b]
wild type	31.5 ± 3.7	
R668A	31.0 ± 1.4	−0.04 ± 0.3
N845A	22.7 ± 1.5	−0.80 ± 0.33
N675A	24.5 ± 0.7	−0.61 ± 0.29
R835L	32 ± 1	0.04 ± 0.3
R836A	27 ± 5	−0.38 ± 0.53
R841A	23 ± 3	−0.77 ± 0.43
N675A/R841A	33.0 ± 1.4	0.11 ± 0.014
K758A	29.0 ± 1.4	−0.20 ± 0.31
Q849A	27 ± 6	−0.38 ± 0.61

[a] Uncertainty values shown are the standard deviation of at least two separate titrations for each protein. [b] Change in the Gibbs free energy of exonuclease site binding of DNA resulting from the protein mutation (calculated from eq 5).

Partitioning of Dansyl-Labeled DNA Substrates between Polymerase and 3′−5′ Exonuclease Sites. Time-resolved fluorescence anisotropy decay experiments were performed to measure the equilibrium distribution of dansyl-labeled DNA substrates between polymerase and 3′−5′ exonuclease sites for each mutant protein. The four different 17-nt primer/27-nt template duplexes used in these experiments, shown in Table 1, contained 0, 1, 2, or 4 consecutive base mismatches. This set of primer-templates was used to assess whether the protein mutations caused different effects on partitioning depending on whether the DNA contained matched or mismatched base pairs. In the wild-type polymerase, duplexes containing increasing numbers of mismatches partition increasingly to the exonuclease site (*16*). In addition, data obtained with quadruply mismatched DNA served to define the fluorescence properties of the exonuclease-bound subpopulation of dansyl probes, necessary to obtain accurate

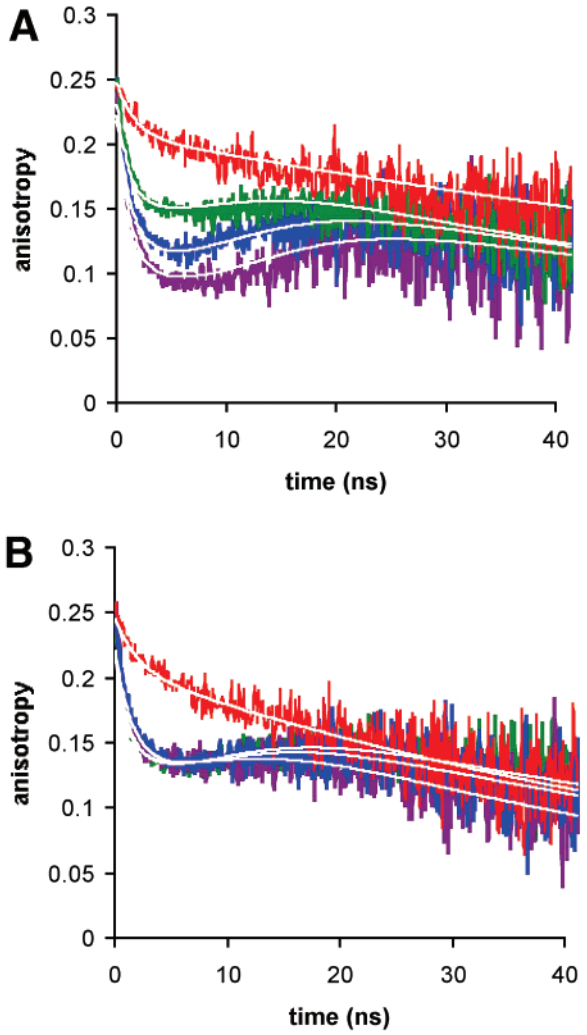

FIGURE 3: Time-resolved fluorescence anisotropy decays of dansyl-labeled DNAs bound to Klenow fragment derivatives. (A) Wild-type Klenow fragment complexes with primer-templates PT0, PT1, PT2, and PT4 (purple, blue, green, and red, respectively). The dip and rise shape, seen particularly in the complexes with one and two mismatch DNAs, indicates a partitioning of the dansyl probe between two distinct environments. (B) Klenow fragment with the N845A polymerase site mutation. Time-resolved decays of PT0, PT1, and PT2 essentially overlay, and the decay associated with four-mismatch-containing DNA (PT4) lies above. In both (A) and (B), the solid fit lines were generated from the known fluorescence behaviors of the two populations, the globally fitted anisotropy parameters associated with the two populations, and the fraction of DNA bound at the exonuclease site, as recovered from the fit. While reported occupancy values in later figures are the average of multiple measurements, the decays and fits portrayed here correspond to a single measurement of a given enzyme/DNA complex.

estimates of the partitioning distribution for the entire data set.

Fluorescence anisotropy decays for each duplex bound to the wild-type polymerase are shown in Figure 3A. A corresponding set of decays for a variant containing an N845A mutation in the polymerase domain is shown in Figure 3B. From these two proteins alone, it is clear that the anisotropy decay for a given DNA/protein complex is distinct and that substrate partitioning is sensitive to the nature of both the DNA substrate and the mutated amino acid residue.

A set of time-resolved anisotropy decays, containing duplicate data sets for each DNA substrate/protein complex, was fitted globally to a two-state model of exposed and buried dansyl probes as described in Materials and Methods. The fit was excellent, as judged by the global reduced χ^2 value of 1.2 as well as by the individual reduced χ^2 values (less than 1.4 for all decays). Since the spectroscopic parameters describing each population were constrained to be the same for each data set, the success of the fit indicates that the characteristics of the exposed and buried probe environments were preserved across the wild-type and all mutant proteins. Previous time-resolved fluorescence anisotropy studies of Klenow fragment/DNA complexes have established that the exposed and buried dansyl probes correspond to distinct subpopulations of bound DNA molecules with their primer termini positioned in the polymerase site or the 3′−5′ exonuclease site, respectively (*15*, *16*). Accordingly, the fraction of exposed dansyl probes recovered from the global analysis is equal to the fraction of DNA bound to the polymerase site at equilibrium.

The fractional occupancies of the polymerase site in each of the DNA/protein complexes are presented graphically in Figure 4. The mutant proteins can be divided into three groups, depending on whether they decrease, increase, or have no effect on the polymerase site occupancy relative to the wild-type Klenow fragment. The first two groups also differ from wild type with respect to their interactions with DNA duplexes containing mismatched base pairs. Each group of mutants is discussed separately below.

The first group of mutant proteins, comprising R668A and N845A, exhibits decreased polymerase site partitioning of correctly base-paired DNA relative to wild type but shows no difference from wild type when the substrate contains a single mismatch at the primer terminus (Figure 4A). In contrast to the wild-type protein, the R668A and N845A mutants are unable to discriminate between duplexes containing a matched or mismatched terminus. These observations indicate that R668 and N845 provide energetically favorable interactions with the duplex that are specific for a correct terminal base pair. When four consecutive mismatched base pairs are present, the DNA is predominantly bound at the exonuclease site for both proteins in this group.

In contrast, proteins in the second group (N675A, R835L, R836A, R841A, and the N675A/R841A double mutant) exhibit increased polymerase site partitioning relative to the wild-type protein for all DNA substrates tested. Results are shown in Figure 4B. Notably, the difference in partitioning relative to the wild-type protein is most pronounced for DNA duplexes containing one or two mismatched base pairs. It is also evident that the double mutation N675A/R841A has a greater effect on polymerase site occupancy than either single mutation. Overall, these mutant proteins do not discriminate between DNAs containing 0, 1, or 2 mismatches; unlike the first group, however, the DNA binds mostly at the polymerase site. Regardless, in each case a DNA duplex containing four terminal mispairs is again bound primarily at the exonuclease site, as seen for the wild-type polymerase and the first group of polymerase site mutants.

The third panel of Figure 4 shows two polymerase mutants (Q849A and K758A) that exhibit pseudo-wild-type behavior. The removal of the K758 side chain yields no significant change in partitioning behavior for DNA substrates with any

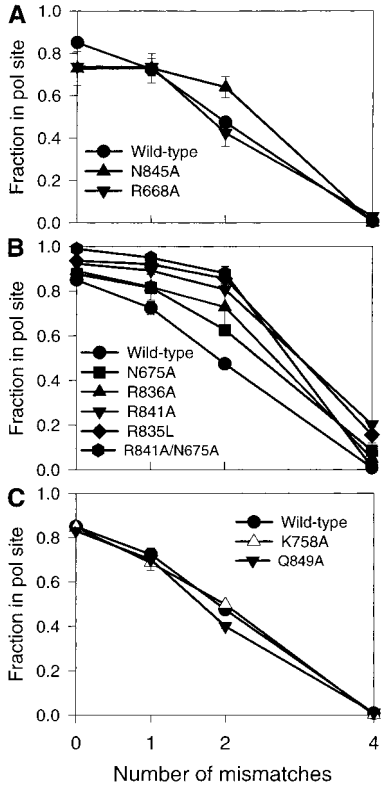

FIGURE 4: DNA partitioning behavior of mutant and wild-type polymerases. (A) Mutants that disrupt recognition of matched base pairs. (B) Mutants that improve polymerase site binding of duplex DNA. (C) Pseudo-wild-type mutants. Fractional polymerase site occupancies as shown are calculated from an average of x_e values (fraction of exposed dansyl probes, corresponding to the fraction of DNA bound to the polymerase site) from multiple measurements of the decay of a given DNA substrate/KF derivative complex. Data for the wild-type Klenow fragment are shown for comparison in all cases. Error bars are standard deviations of two or more experimental values. In some cases, the error bars are smaller than the symbols used to represent experimental data points.

number of mismatches, consistent with structural data showing that this side chain does not interact with the DNA primer-template in either the polymerase or exonuclease modes of binding (*4*−*6*, *25*). Interestingly, removal of the Q849 side chain also has little effect on binding of any of the primer-templates, even though this side chain appears to make a direct DNA contact in the cocrystal structures of homologous DNA polymerases bound to DNA substrates (*4*−*6*).

To assess the energetic consequences of changes in polymerase site occupancy, $\Delta\Delta G°_{pol}$ values were calculated for each mutant protein according to eq 12 in the Materials and Methods section. Under this definition, $\Delta\Delta G°_{pol}$ quantifies the change in the Gibbs free energy of binding DNA at the polymerase site resulting from a mutation to the protein. A positive $\Delta\Delta G°_{pol}$ value indicates that a mutation destabilizes binding of the DNA substrate at the polymerase site, whereas a negative value indicates that a mutation has a stabilizing effect on polymerase site binding. Generally, the $\Delta\Delta G°_{pol}$ values depend on the position of the protein mutation(s) and the type of DNA substrate used (Table 3).

In calculating the $\Delta\Delta G°_{pol}$ values in Table 3, it was assumed that the $\Delta\Delta G°_{exo}$ term in eq 12 is the same for all duplexes (containing 0−2 mismatches) and is equal to the value obtained from the exonuclease site binding titrations

Table 3: $\Delta\Delta G°_{pol}$ Values[a] for Klenow Fragment Derivatives

pol site mutation	no. of mismatches		
	0	1	2
R668A	1.7 ± 0.5	−0.2 ± 0.6	0.5 ± 0.7
N845A	1.4 ± 0.8	−0.9 ± 0.8	−2.3 ± 0.4
N675A	−1.2 ± 0.9	−1.9 ± 0.5	−2.1 ± 0.3
R835L	−2.3 ± 1.4	−3.6 ± 0.8	−4.6 ± 0.5
R836A	−1.2 ± 0.8	−1.7 ± 1.0	−3.0 ± 1.1
R841A	−2.6 ± 0.6	−3.6 ± 0.6	−4.5 ± 0.5
N675A/R841A	−6.8 ± 2.5	−5.3 ± 0.7	−5.0 ± 0.9
K758A	−0.1 ± 0.6	0.2 ± 0.6	−0.4 ± 0.4
Q849A	0.01 ± 0.7	0.09 ± 0.7	0.4 ± 0.8

[a] $\Delta\Delta G°_{pol}$ values are calculated from eq 12 and are expressed in kJ/mol.

(obtained for a duplex with four mismatches). This should be a reasonable approximation because the primer terminal sequence is the same in all duplexes, and it is this portion of the DNA substrate that binds at the exonuclease site as a single strand. The uncertainties in the $\Delta\Delta G°_{pol}$ values listed in Table 3 reflect the propagated error from both the dansyl partitioning measurements and the DNA binding titrations.

DISCUSSION

Many of the amino acid side chains within the polymerase domain of the Klenow fragment are highly conserved across bacterial DNA polymerases, pointing to their important roles in one or more aspects of polymerase function. Previous studies have identified side chains involved in binding duplex DNA substrates at the polymerase active site (*9*), in selection and binding of appropriate nucleotide substrates (*13*, *14*), and in catalysis of the nucleotidyl transfer reaction (*8*, *9*). Another potential role of polymerase site side chains is in identification of mismatched DNA base pairs resulting from base misincorporation events. To ensure high replication fidelity, a mismatched terminus must be recognized at the polymerase site and then transferred to the exonuclease site for removal of the misincorporated base. In this study, we have identified six polymerase domain mutations that compromise the ability of the Klenow fragment to discriminate between DNA substrates that contain matched or mismatched base pairs. Four of the mutated side chains (R668, N675, R841, and N845) are invariant in 50 bacterial polymerases, and another (R836) is well conserved as a positive charge (R or K).[1]

A duplex DNA substrate bound to the Klenow fragment naturally partitions between the separate polymerase and 3′−5′ exonuclease sites. In the wild-type enzyme, this partitioning is sensitive to the presence of mismatched base pairs within the DNA (*16*, *17*). Mutations within the polymerase domain also affect the partitioning behavior, as shown in this study. In principle, a change in partitioning could be due to alterations in DNA binding at either the polymerase or exonuclease sites. However, the results of the exonuclease site binding titrations indicate that none of the mutations significantly affect binding of DNA to the exonuclease site (Table 2). The crystal structure of an editing complex of the Klenow fragment with duplex DNA (*25*) reveals that six of

[1] The DNA polymerase sequence alignments on which these conclusions are based are available at http://pantheon.yale.edu/~cjoyce/align.html.

the side chains examined here (R668, K758, R836, R841, N845, and Q849) are not in proximity to the DNA substrate (Figure 1A) and, therefore, would not be expected to perturb exonuclease site binding. Interestingly, two side chains (N675 and R835) do appear to interact with the DNA substrate, through contacts with phosphate groups in the primer or template strands. Apparently, these interactions contribute little or no binding energy for a DNA substrate bound at the exonuclease site.

In view of the above discussion, it is evident that the mutations examined here primarily affect the binding of DNA substrates at the polymerase site. The $\Delta\Delta G^{\circ}_{pol}$ values (Table 3) measure the effect of the mutations on the thermodynamic stability of the polymerase site DNA/protein complex. These values therefore reflect the energetic contributions to DNA binding of individual protein side chains within the polymerase domain. It is desirable to interpret these data in relation to a crystal structure of the complex. Unfortunately, a crystal structure of the Klenow fragment with duplex DNA at the polymerase site has not been solved. The high-resolution structure of the large fragment of the *Bst* polymerase with duplex DNA at the polymerase site (*4*) provides an appropriate model, however, because this fragment is analogous to the Klenow fragment and there is a very high degree of sequence homology between the two proteins. The *Bst* polymerase cocrystal was obtained by crystallizing the enzyme with duplex DNA in the absence of nucleotide substrates and should therefore correspond to the binary complex of the Klenow fragment and duplex DNA used in our solution experiments. The positioning of the DNA duplex in this structure (Figure 1B) is also very similar to that seen in complexes of Klentaq polymerase or T7 DNA polymerase with DNA (*5*, *6*).

Recognition of Correct Base Pairs. Our results indicate that R668 and N845 function in recognition of matched Watson−Crick base pairs at the primer terminus of a duplex DNA substrate bound at the polymerase active site. Mutation of either residue disrupts polymerase site binding when the duplex terminus is matched but not when it is mismatched (Figure 4A and Table 3), indicating that the side chains of these residues provide favorable binding interactions that are specific for a matched terminal base pair. Structural indications of favorable interactions between the DNA substrate and the side chains of R668 and N845 are evident in the cocrystal structures mentioned above.

In these structures, the homologue of R668 makes a direct hydrogen bond contact with the minor groove edge of the primer-terminal base (*4*−*6*). Hydrogen bond acceptors in the minor groove (N3 of purines, O2 of pyrimidines) are in similar geometric positions in the four correct base pairs but are differently positioned in mismatched base pairs (*26*), and this geometric specificity has been invoked as one means by which mismatched base pairs could be differentiated from matched base pairs. The minor groove hydrogen bond would explain why R668 provides favorable binding energy when the primer terminus is correctly base paired. Therefore, either a mismatched terminus or mutation of the R668 side chain would be expected to disrupt this favorable interaction. Accordingly, either modification should produce a similar change in polymerase site occupancy. Moreover, the presence of both modifications should not produce an effect beyond that of either one alone. Thus, our results (Figure 4A and Table 3) are entirely consistent with a minor groove hydrogen bond.

In the cocrystal structures, the side chain equivalent to Q849 makes a direct minor groove hydrogen bond to the template base opposite the primer terminus. Thus, Q849 might also be expected to provide favorable binding energy for a matched DNA duplex at the polymerase site. In fact, our results for the Q849A mutant indicate that the energetic contribution of this side chain is negligible (Table 3). More strikingly, despite the apparent similarity of the roles of Q849 and R668, mutation of Q849 did not impair discrimination between a matched and mismatched substrate (Figure 4C). These results are consistent with kinetic studies with primer-templates containing chemically modified bases (*27*), which showed that extension of a DNA substrate by the Klenow fragment required a hydrogen bond acceptor at the primer terminus but that an acceptor on the corresponding template base was less important. These results suggest that minor groove hydrogen bond contacts to the primer-terminal base are energetically more important than contacts to the opposing template base. The different energetic contributions of R668 and Q849 have been directly quantified in the present study (Table 3).

Our results for the N845A mutant protein, together with structural data from homologous polymerases, suggest that N845 functions in a manner different from R668, even though both side chains are involved in recognition of matched terminal base pairs. The cocrystal structures show that the homologue of N845 does not interact directly with the terminal base pair but instead forms a hydrogen bond with the sugar ring of the template nucleotide at this position (*5*, *6*). If the DNA backbone became mispositioned by a mispair, this interaction would be lost. Thus N845 may recognize a matched terminal base pair by an indirect mechanism that depends on the proper geometry of the DNA backbone.

At this time, it is difficult to test this prediction, as no structures of polymerases with mismatched DNA substrates have currently been solved. However, our results do indicate that the favorable energetic contribution of N845 is lost when the DNA terminus is mismatched. In fact, the contribution of N845 is slightly destabilizing when a single mismatch is present (Table 3), although the effect may not be significant in view of the uncertainty in the $\Delta\Delta G^{\circ}_{pol}$ value. However, the unfavorable binding energy is magnified when two mismatches are present at the DNA terminus. Presumably, the structural distortion of the DNA backbone resulting from the mismatches causes a steric clash with N845. Thus, in addition to recognizing a matched terminal base pair, N845 may also discriminate against mismatches at the DNA terminus.

An additional role for the N845 side chain is suggested by the crystal structure of the ternary complex of T7 DNA polymerase, duplex DNA, and nucleotide substrate, where the side chain of N845 makes a water-mediated minor groove hydrogen bond with the nucleotide, as well as the previously mentioned hydrogen bond with the sugar ring of the template base opposite the primer terminus (*6*). While probably not relevant to our binary system, this interaction is consistent with previous work showing that the N845A mutation yields an increase in the K_m(dNTP) relative to wild-type polymerase and a mutator phenotype in fidelity assays (*9*, *11*).

Side Chains That Interact Unfavorably with DNA. The group of mutants comprising N675A, R835L, R836A, and R841A actually improve binding of DNA at the polymerase site relative to wild type (Figure 4B). The side chains of these residues might therefore be involved in distorting the duplex DNA substrate, making binding at the polymerase site less favorable. Alternatively, the negative energetic contribution to substrate binding at the polymerase site might reflect an unfavorable orientation of the side chain itself: a distortion of the protein structure upon DNA binding. In either case, it would appear that the removal of the side chain results in a lesser distortion of the DNA substrate or of the protein itself and, therefore, more favorable polymerase site binding.

Notably, the unfavorable binding energy associated with each residue is significantly larger when the duplex contains one or, especially, two terminal mismatches (Table 3). This could indicate that the mismatches induce additional strain in the protein, perhaps through steric clashes, or that the mispaired duplexes are less able to accommodate the conformational distortion imposed by the protein. Regardless of the mechanism used, these residues appear to discriminate against mismatched base pairs in the DNA substrate.

Interestingly, our results for the N675A/R841A double mutant derivative indicate that the unfavorable energetic contributions of N675 and R841 sum in an additive fashion (Table 3). Thus, while the contribution of individual residues is relatively small, the total strain energy stored in the DNA and/or protein backbone is much larger.

The notion that significant strain is exerted on the duplex in the polymerase active site is supported by structural data. Crystal structures of various polymerases show that DNA bound to the polymerase domain exhibits an S-shaped "kink" and that, close to the active site, the structure of the DNA is distorted from B- to A-form (*5*, *6*, *24*, *28*). In fact, in the *Bst*, Klentaq, and T7 polymerases, the residue homologous to N675 interacts with the template strand at the position where the DNA switches from B-form to A-form geometry; thus, N675 may be responsible, in part, for imposing this conformational distortion in the DNA, consistent with the unfavorable DNA binding energy contributed by this residue. Such a role may explain the high sequence conservation of N675 within the Pol I family.

The side chains of R835, R836, and R841 appear to be positioned to interact with the single-stranded portion of the template. Cocrystal structures of homologous DNA polymerases bound to DNA substrates show that the template strand is sharply bent just beyond the primer terminus (*5*, *6*). The side chains of R835, R836, and R841 may help to enforce this distortion, accounting for the unfavorable energetic contribution to DNA binding. In fact, R841 interacts with the phosphate backbone at the point where the template strand is sharply bent, and in ternary complexes containing both DNA and nucleotide substrates, this residue also interacts with a flipped template base (*5*, *6*).

Unfortunately, none of the available crystal structures provide information on the interactions that R835 and R836 make with the DNA substrate. The homologues of these residues are further away from the primer terminus (Figure 1B), but none of the available structures show a sufficient number of unpaired template bases to discern the interactions involved. Nonetheless, our results strongly suggest that these residues make direct contacts to the DNA substrate.

Mismatch Discrimination and Polymerase Fidelity. Clearly, the polymerase domain of the Klenow fragment is not optimized for binding duplex DNA, as mutations of N675, R835, R836, and R841 all lead to tighter binding. What is the role of these residues in polymerase function? One possibility is that the unfavorable binding energy contributed by these residues is required to optimize the chemistry of nucleotide incorporation. Alternatively, these residues may distort the duplex DNA substrate in order to discriminate between matched and mismatched base pairs. This role is strongly suggested by our results, which indicate that mutations in these residues compromise the ability of the enzyme to discriminate matched from mismatched terminal base pairs. The structural distortion could position the critical regions of the duplex in proper juxtaposition relative to specificity-determining side chains of the enzyme. Discrimination between matched and mismatched base pairs could then occur through hydrogen bond contacts in the minor groove of the duplex. The distortion of the DNA duplex may also bring the binding affinity of the polymerase site into a range where the partitioning of the primer terminus between the polymerase and exonuclease sites is most sensitive to the presence of mismatches. If binding to the polymerase site is too tight, then a mismatch will have little effect on how much DNA partitions into the exonuclease site. Thus, a tight binding polymerase site would be deleterious for proofreading of misincorporation errors.

Following a misincorporation event at the polymerase site, the primer terminus must be transferred to the exonuclease site for removal of the mismatched base. In principle, the decision to edit could occur immediately after misincorporation or after the primer terminus has translocated to a "preaddition" position in the polymerase active site, in readiness for the next cycle of nucleotide binding and incorporation. Structural studies of a catalytically active *Bst* polymerase/DNA cocrystal indicated that, following nucleotide incorporation, the primer terminus occupies the same preaddition" position as in a binary enzyme/DNA complex (*4*). This observation suggests that translocation occurs rapidly after nucleotide incorporation. Hence, the decision to edit is probably made from a complex that resembles the binary enzyme/DNA complex used in our experiments. Accordingly, side chains identified here as determinants of mismatch discrimination may play a key role in the editing decision.

CONCLUSIONS

This study has demonstrated the utility of time-resolved fluorescence anisotropy in probing a portion of the polymerase reaction cycle previously difficult to study: the decision step following nucleotide incorporation but preceding further polymerization or excision. Several residues within the polymerase domain have been identified as affecting the identification of matched versus mismatched base pairs within the DNA substrate. Hence, this recognition is not solely dependent on the thermodynamic differences between matched and mismatched base pairs. The side chains of R668 and N845 appear to provide favorable interactions with a correctly paired DNA terminus, thereby stabilizing the

binding of the DNA substrate at the polymerase site. In contrast, the side chains of N675, R835, R836, and R841 appear to discriminate against the binding of a mispaired primer terminus to the polymerase active site. Through the combined effect of these residues, a correctly base-paired substrate will be retained at the polymerase active site, while a mismatched duplex is more likely to be rejected from the site and instead bind at the exonuclease site. Such a combined effect may be seen with the N675A/R841A double mutant, which results in significantly greater polymerase site partitioning than is produced by either mutation alone. Thus, the residues identified in this study are likely to play important roles in the proofreading mechanism of the Klenow fragment.

While the proximity of these side chains to DNA substrates bound at the polymerase site is clearly apparent from the crystal structures, the structural data do not provide information on the energetic contributions of protein side chains, which can be either favorable or unfavorable. Moreover, the function of the side chains in mismatch recognition and discrimination could not be inferred from the structural data. Our analysis of the DNA partitioning equilibrium in the wild-type and mutant proteins, therefore, provides complementary information on the workings of a polymerase that would not have been available from crystal structures or biochemical studies alone.

ACKNOWLEDGMENT

We thank Xiaojun Chen Sun for construction of Klenow fragment mutations and expression plasmids.

REFERENCES

1. Brutlag, D., Atkinson, M. R., Setlow, P., and Kornberg, A. (1969) *Biochem. Biophys. Res. Commun. 37*, 982−929.
2. Dahlberg, M. E., and Benkovic, S. J. (1991) *Biochemistry 30*, 4835−4843.
3. Kuchta, R. D., Benkovic, P., and Benkovic, S. J. (1988) *Biochemistry 27*, 6716−6725.
4. Kiefer, J. R., Mao, C., Braman, J. C., and Beese, L. S. (1998) *Nature 391*, 304−307.
5. Li, Y., Korolev, S., and Waksman, G. (1998) *EMBO J. 17*, 7514−7525.
6. Doublié, S., Tabor, S., Long, A. M., Richardson, C. C., and Ellenberger, T. (1998) *Nature 391*, 251−258.
7. Steitz, T. A. (1999) *J. Biol. Chem. 274*, 17395−17398.
8. Polesky, A. H., Dahlberg, M. E., Benkovic, S. J., Grindley, N. D. F., and Joyce, C. M. (1992) *J. Biol. Chem. 267*, 8417−8428.
9. Polesky, A. H., Steitz, T. A., Grindley, N. D. F., and Joyce,C. M. (1990) *J. Biol. Chem. 265*, 14579−14591.
10. Bell, J. B., Eckert, K. A., Joyce, C. M., and Kunkel, T. A. (1997) *J. Biol. Chem. 272*, 7345−7351.
11. Minnick, D. T., Bedenek, K., Osheroff, W. P., Turner, R. M. Jr., Astatke, M., Liu, L., Kunkel, T. A., and Joyce, C. M. (1999) *J. Biol. Chem. 274*, 3067−3075.
12. Astatke, M., Ng, K., Grindley, N. D. F., and Joyce, C. M. (1998) *Proc. Natl. Acad. Sci. U.S.A. 95*, 3402−3407.
13. Astatke, M., Grindley, N. D. F., and Joyce, C. M. (1998) *J. Mol. Biol. 278*, 147−165.
14. Astatke, M., Grindley, N. D. F., and Joyce, C. M. (1995) *J. Biol. Chem. 270*, 1945−1954.
15. Guest, C. R., Hochstrasser, R. A., Dupuy, C., Allen, D. J., Benkovic, S. J., and Millar, D. P. (1991) *Biochemistry 30*, 8759−8770.
16. Carver, T. E., Hochstrasser, R. A., and Millar, D. P. (1994) *Proc. Natl. Acad. Sci. U.S.A. 91*, 10670−10674.
17. Carver, T. E., and Millar, D. P. (1998) *Biochemistry 37*, 1898−1904.
18. Lam, W. C., Van der Schans, E. J. C., Joyce, C. M., and Millar, D. P. (1999) *Biochemistry 38*, 2661−2668.
19. Lam, W. C., van der Schans, E. J. C., Joyce, C. M., and Millar, D. P. (1998) *Biochemistry 37*, 1513−1522.
20. Allen, D. J., Darke, P. L., and Benkovic, S. J. (1989) *Biochemistry* 28, 3612−3621.
21. Derbyshire, V., Freemont, P. S., Sanderson, M. R., Beese, L., Friedman, J. M., Joyce, C. M., and Steitz, T. A. (1988) *Science 240*, 199−201.
22. Joyce, C. M., and Derbyshire, V. (1995) *Methods Enzymol. 262*, 3−13.
23. Bailey, M. F., Thompson, E. H. Z., and Millar, D. P. (2001) *Methods 25*, 62−77.
24. Eom, S. H., Wang, J., and Steitz, T. A. (1996) *Nature 382*, 278−281.
25. Beese, L. S., Derbyshire, V., and Steitz, T. A. (1993) *Science 260*, 352−355.
26. Seeman, N. C., Rosenberg, J. M., and Rich, A. (1976) *Proc. Natl. Acad. Sci. U.S.A. 73*, 804−808.
27. Morales, J. C., and Kool, E. T. (2000) *Biochemistry 39*, 12979−12988.
28. Pelletier, H., Sawaya, M. R., Kumar, A., Wilson, S. H., and Kraut, J. (1994) *Science 264*, 1891−1903.
29. Christopher, Jon A. (1998) *SPOCK: The Structural Properties Observation and Calculation Kit (Program Manual)*, The Center for Macromolecular Design, Texas A&M University, College Station, TX.

BI0114271